Neutron Diffraction Studies of Graphite−Potassium−Methylamine: Staging Transitions and Structure of New Graphite Intercalation Compounds

Neal T. Skipper,* Jennifer K. Walters, Colin Lobban, Jane McKewn, Robin Mukerji, Gary J. Martin, and Michael de Podesta

Department of Physics and Astronomy, University College, Gower Street, London WC1E 6BT, U.K.

Alex. C. Hannon

ISIS Facility, Rutherford Appleton Laboratory, Chilton, Didcot, OXON OX11 OQX, U.K.

Received: August 10, 2000

Graphite intercalation compounds (GICs) of the type $KC_x(CH_3NH_2)_y$ have been prepared by in situ amination of stage-II $C_{24}K$ and stage-IV $C_{48}K$, and studied by time-of-flight neutron diffraction. As the vapor pressure of methylamine is increased the compounds pass through a rich sequence of staging transitions, in which the regular repeat of *n* empty graphite layers is progressively filled by intercalant. In these staging transitions, *n* always changes by −1. We therefore observe lower stage *unaminated* compounds as methylamine is introduced into the starting compounds. Isotopic substitution of CD_3ND_2 for CD_3NH_2 has enabled us to determine the detailed structure of the fully aminated stage-I and stage-II end compounds, $C_{24}K(CH_3NH_2)_3$ and $C_{48}K(CH_3NH_2)_3$. We find that the interlayer structure is based on 3-fold coordinated potassium ions and is relatively insensitive to the stage.

Introduction

Graphite intercalation compounds (GICs) are an important class of materials that have many practical applications,[1] and allow us to study a variety of low-dimensional phenomena.[2−4] In addition to novel structural, dynamic, and electronic properties, GICs also appear to be unique in that a series of stoichiometric compositions can be obtained with a given intercalant species.[4] These compositions give rise to a series of *c*-axis superlattices, in which an integral number (known as the *stage*) of graphene sheets separate nearest intercalant layers.

Ternary graphite intercalation compounds (GICs) of the type $C_xK(NH_3)_y$ pass through a rich sequence of stages and intercalant structures as ammonia content, *y*, is increased.[5−8] In addition, experimental studies of $K(NH_3)_xC_{24}$ with compositions in the range $0 < x < 4.38$ have identified two important electronic transitions.[6,7] First, in the range $0.05 < x < 1.0$ resistance perpendicular to the graphite layers increases by 2 orders of magnitude. This increase coincides with the conversion of a stage-II GIC to a stage-I GIC, with a repeat distance of 6.6 Å. Second, as $x > 4.0$, resistance in the plane of the graphite layers first increases, and then shows a notable but shallow decrease. This is seen as evidence for a 2-dimensional nonmetal−metal transition in the intercalant layers, caused by back transfer of electrons from the host graphite once the potassium has been fully solvated by four ammonia molecules. This leads to the expectation that metal−ammonia GICs are the two-dimensional structural and electronic analogues of the bulk metal−ammonia solutions. There are therefore strong reasons for exploring the existence and structure of graphite−potassium−methylamine GICs.

Unlike their ammonia counterparts, bulk metal−methylamine solutions do not exhibit a true composition driven metal−
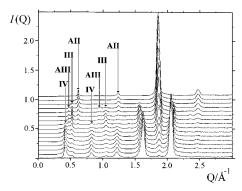
nonmetal transition.[9] This reluctance to form a metallic state is attributed to localization of electron pairs within cation cavities, resulting in, for example, $e^−−K^+−e^−$ species.[10] The opportunity therefore exists for employing $K(NH_3)_xC_{24}$ and $K(CH_3NH_2)_xC_{24}$ systems to study the effects of dimensionality on electron localization and the metal−nonmetal transition, in the crossover regime between 2-dimensional and 3-dimensional behavior.

Neutron diffraction techniques have already been successful in determining detailed structure in staged potassium-ammonia GIC systems.[5,6] In this context, neutrons have the important advantages of "seeing" light elements, and providing the opportunity to exploit isotopic substitution methods. For example, both hydrogen (H) and its isotope deuterium (D) scatter neutrons strongly. In addition, the neutron scattering lengths, *b*, of H and D have different signs: $b_H = −3.74$ fm and $b_D = 6.67$ fm. Isotope substitution of D for H, applied in conjunction with difference analysis, can therefore be used to locate hydrogen atoms unambiguously.[6] In this paper we apply this technique to study for the first time the staging transitions and structure of compounds of the type $KC_x(CH_3NH_2)_y$.
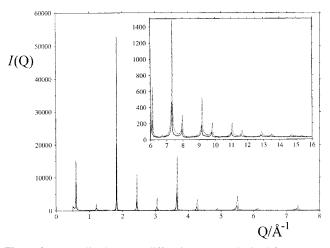
Experimental Details

The samples were prepared using the "one zone" method described in Carlile et al.[11] for Cs GICs. A 1 cm^2 by ∼0.5 mm thick piece of highly oriented pyrolytic graphite (HOPG) was placed in the Pyrex reaction tube together with an excess of potassium metal. Previously the HOPG had been outgassed for ∼12 h at 350 °C under a vacuum of $10^{−5}$ mbar. The reaction tube was then heated to 300 or 360 °C, and held at that temperature for ∼24 h. After this time, the graphite had taken on a metallic blue-purple color, indicating the formation of either stage-II or stage-IV K-GIC. These starting materials have nominal compositions KC_{24} and KC_{48}, respectively. X-ray and neutron data for the starting K-GICs confirm that the compounds

* Corresponding author. E-mail: n.skipper@ucl.ac.uk.

Figure 1. Staging transitions during the methylamination of stage-IV $C_{48}K$. Uncorrected neutron diffraction patterns are shown as a function of CD_3NH_2 pressure, at intervals of 0.2 bar up to 3 bar. Compounds are stage-IV KC_{48} (IV = 15.45 Å), stage-III KC_{36} (III = 12.10 Å), aminated stage-III (AIII = 13.59 Å), and aminated stage-II (AII = 10.30 Å). Patterns were allowed to equilibrate after each change in vapor pressure, for approximately 30 min.
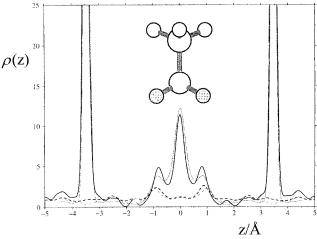

Figure 2. Normalized neutron diffraction pattern obtained from stage-II $C_{48}K(CD_3NH_2)_3$, showing the (00l) series of Bragg peaks (Table 1). The c^*-axis spacing of this material is 10.30 Å. The sample was oriented so that the scattering vector, **Q**, was parallel to the c^*-axis. Data were collected at a methylamine pressure of 3 bar, into two detector banks at $\theta = 35°$ and $\theta = 150°$. Data are shown for two isotopically labeled samples: CD_3ND_2 (solid line), and CD_3NH_2 (dotted line). The insert shows the high-Q data obtained from the 150° bank, registering peaks up to $l = 16$.

were predominantly stage-II ($d = 8.75$ Å) or stage-IV ($d = 15.45$ Å), with minor contamination due to a stage-III ($d = 12.10$ Å) component (see Figure 1).

The starting sample was then transferred to a purpose built cylindrical sample container, manufactured from null scattering Ti/Zr alloy, for in situ solvation with isotopically labeled methylamine vapor. The amount of methylamine absorbed by the K-GIC is determined by the applied vapor pressure: at 3 bar the composition is found to be $KC_x(CH_3NH_2)_3$. It is worth noting here that intercalation with methylamine is not a reversible process, and that residual compounds obtained by vacuum pumping still contain a small amount of amine.

Initially the potassium−GIC samples were exposed to increasing CD_3NH_2, in steps of 0.2 bar up to 3 bar (Figure 1). At each point we waited until equilibration of the total diffraction pattern had been achieved, typically 30 min. For the final compound, data were then collected over a period of approximately 8 h into each of the two detector banks. The can was then evacuated for ~4 h before CD_3ND_2 was introduced, gradually increasing the pressure to 3 bar. After 1 h a second

Figure 3. Neutron scattering density profiles, $\rho(z)$, for the stage-II $C_{48}K(CD_3NH_2)_3$ (heavy lines) and stage-I $C_{24}K(CD_3NH_2)_3$ (light lines) obtained by inverse Monte Carlo fitting to the relative peak intensities of eq 1 and Table 1.[13] Due to our use of H/D isotope substitution we are able to locate the interlayer $-NH_2$ protons. The solid lines show all species except those labeled by H/D substitution, the dashed lines those labeled by H/D substitution. The profiles shown are in arbitrary units, but can be normalized to neutron scattering density by comparing with the known chemical composition of the graphite layers (see Table 2). The total R factor for the fit to the integrated intensity data is ~3%. The molecular graphics model of methylamine shows a possible orientation of the intercalated molecule.

exchange was then executed. Data were collected for this K-GIC for approximately 8 h, as before.

The neutron diffraction data presented here were collected on the ISIS pulsed neutron source at the Rutherford Appleton Laboratory (UK) using the liquid and amorphous diffractometer, LAD.[12] Neutrons are scattered from the sample orientated with the c^*-axis parallel to the scattering vector, **Q**, into fixed angle detectors. To obtain a complete scattering profile, data from detectors at 35° and 150° were combined (Figure 2). The scattered intensity is measured at the detectors as a function of time-of-flight (ToF), which can be directly related to the scattering vector. Monitors record the ToF spectra of the incident and transmitted beams to provide information on the total neutron cross section and the intensity:wavelength profile of the incident beam.

For each experiment, measurements are required for the sample, the empty sample container, a background without sample or container, and a vanadium rod of comparable geometry to the sample container. This last measurement allows the sample scattering to be put on an absolute scale, since vanadium has a well-known and almost entirely incoherent scattering cross section. The corrections applied to the data are for background and container scattering. Multiple scattering and attenuation effects are expected to be small and the same for all spectra; therefore, as only relative peak intensities are required, these corrections were deemed unnecessary.

In this neutron diffraction experiment we recorded the scattering perpendicular to the graphite planes, i.e., along the c^*- or z-axis. This allows us to measure the (00l) series of Bragg peaks, at positions determined by the repeat sandwich thickness of the compound, d. The intensities of the (00l) Bragg peaks were determined by fitting the data with split-Pearson VII [20] shaped peaks. This function was chosen because it can fit to asymmetric, overlapping, peaks. The data were fitted in sections containing 4−6 Bragg peaks, and the integrated areas were then evaluated by a Simpson's rule integration of the fitted peak

Letters

J. Phys. Chem. B, Vol. 104, No. 47, 2000 **10971**

TABLE 1: Peak Positions and Relative Peak Intensities of the First 16 (00*l*) Bragg Peaks, for Stage-II Potassium−Methylamine Graphite Intercalation Compounds under 3 bar of Methylamine Pressure, Evaluated from the Split-Pearson VII Bragg Peak Fitting[a]

	$I(Q)$	
$Q/\text{Å}^{-1}$	$C_{48}K(CD_3ND_2)_3$	$C_{48}K(CD_3NH_2)_3$
0.61	0.1930	0.275
1.22	0.0392	0.0415
1.83	1.0	1.0
2.44	0.0951	0.0880
3.05	0.0440	0.033
3.66	0.1616	0.1833
4.27	0.0529	0.0513
4.88	0.0099	0.0073
5.49	0.0980	0.0966
6.10	0.01738	0.0208
6.71	0.0	0.0
7.32	0.0814	0.0574
7.93	0.00925	0.00733
8.54	0.000148	0.0
9.16	0.01886	0.0171
9.76	0.00703	0.00611

[a] The (001) and (002) Bragg reflections were obtained from the detector bank at 35°, the remainder from the bank at 150°. The (003) reflection is used as the normalization point of the intensities.

profile. Data from the 35° detectors were scaled to those at 150° by comparing the overlay region.

For the pure stage-I and stage-II aminated compounds the neutron scattering densities along the *z*-axis, $\rho(z)$, were obtained by inverse Monte Carlo fitting to the integrated Bragg peak intensities, $I(Q)$.[13] These are related to $\rho(z)$ via the structure factor, $F(Q)$:

$$I(Q) = M(Q)|F(Q)|^2 \qquad (1)$$

$$F(Q) = \int_{-d/2}^{d/2}\rho(z)e^{iQz}\,\mathrm{d}z \qquad (2)$$

where *d* refers to the smallest repeat distance along the *c**-axis. $M(Q)$ is a *Q*-dependent form factor, which takes into account the mosaic spread and finite size of the sample, and the Debye−Waller factor.[13] Because of the H/D substitution on CD_3NH_2, we are able to isolate the distribution amine group hydrogen atoms from the other components, as shown in Figure 3.

Results and Discussion

We begin by identifying the GICs that have been observed during our experiments. The compounds, with label and *c*-axis

spacing in brackets, are; stage-IV KC_{48} (IV = 15.45 Å), stage-III KC_{36} (III = 12.10 Å), stage-II KC_{24} (II = 8.75 Å), stage-I KC_8 (I = 5.40 Å), methylaminated stage-III $KC_{72}(CH_3NH_2)_x$ (AIII = 13.59 Å), methylaminated stage-II $KC_{48}(CH_3NH_2)_x$ (AII = 10.30 Å) and methylaminated stage-I $KC_{24}(CH_3NH_2)_x$ (AI = 6.95 Å). The methylamine content depends on the applied vapor pressure, with $x \leq 3$.

Scattering data collected during the methylamination of IV are shown in Figure 1. We note first that we do not see AIV, which would have a layer spacing of 16.98 Å, and (001) and (002) Bragg peaks at 0.37 and 0.74 Å^{-1}. Instead, the starting compound is first converted to III and AIII. The formation of a lower stage *unaminated* compound during amination is at first sight surprising, but is presumably required to conserve overall K^+ content within the constraint of stoichiometric staged compounds. The methylamine content of our AIII cannot be determined from the current experiments. However, the fact that it is soon converted to AII suggests that the K^+ ions are not fully solvated by three methylamine molecules. At vapor pressures greater than 1.0 bar AII appears, and is the only component in the final compound formed at 3 bar. We therefore conclude that the only allowed staging transitions allowed during methylamination have $\Delta n = -1$, where Δn is the change of stage. This rule applies even if the transition involves amination/demamination. For this reason we did not see AIV or II during conversion of IV to AII. In contrast, transitions with $\Delta n = 0$ (for example II to AII) have been observed during *ammoniation* of K-GICs.[7] This is probably due to the smaller size of ammonia, which allows the molecule to intercalate without reorganization of the in-plane K^+ structure.[8]

Peak positions and relative intensities for the final AII compound are given in Table 1, and are displayed graphically in Figure 2. The data for the two isotopically distinct samples, $KC_{48}(CD_3ND_2)_3$ and $KC_{48}(CD_3NH_2)_3$, reveal quite large changes in the relative intensities of the Bragg peaks due to isotopic substitution. The density profiles obtained from the intensity data for AII and AI are shown in Figure 3. These profiles are zeroed on the center of the interlayer region, to allow us to compare the two samples more easily. The plots show the unsubstituted scattering length density profiles (all atomic species except the isotopically substituted H/D) and the difference profiles (only the isotopically substituted H/D atoms).

Considering first the isotope independent profiles (solid lines), there are sharp peaks at ±6.825 and ±3.475 Å due to the flat (unrumpled) graphite layers, with the peaks at ±6.825 Å of course being present in AII but not AI. The area under these

TABLE 2: Structure of Stage-II (*d* = 10.30 Å) and Stage-I (*d* = 6.95 Å, in Italics) Potassium−Methylamine−Graphite, at 3 bar of Methylamine and Room Temperature[a]

density profile	peak position/Å	peak area	assignment	comment
H/D isotope independent (solid lines)	±6.825	15.95	1.0 C_{24}	peaks used to normalize the distribution
	±3.475	*15.95*	1.0 C_{24}	
		15.95	*1.0 C_{24}*	
	−0.800	2.65	K + 3.12 (CD_3N)	we assume that K is conserved,
		2.47	*K + 3.29 (CD_3N)*	and that H/D substitution was complete
	0.000	6.28		
		7.27		
	+0.800	2.66		
		2.49		
H/D isotope dependent (dashed lines)	−0.900	2.00	3.00 D	we assume H/D substitution is complete, and assign protons the scattering length of D
		2.28	*3.43 D*	
	+0.900	2.05	3.07 D	
		2.30	*3.48 D*	

[a] Peak positions and peak areas were obtained from the neutron scattering density profiles such shown in Figure 3. The neutron scattering lengths, *b*, for relevant species are C = 0.6646 fm, K = 0.367 fm, N = 0.937 fm, H = −0.3739 fm, D = 0.6671 fm

peaks corresponds to C_{24}, and is used to normalize other features in the data (Table 2). In the center of the interlayer region there is a peak that we attribute to approximately collinear K^+, C, N, and D(C). The side shoulders at ± 0.8 Å are then due to (rotationally hindered) D(C). In both samples, the data are consistent with solvation of K^+ by approximately three methylamine molecules.

The isotope-dependent H/D profiles locate the labeled protons in two broad peaks at ± 0.9 Å, whose areas are again consistent with approximately three methylamine molecules per K^+. The separation of these peaks is greater than the intramolecular H−H(N) separation, and implies that the $-NH_2$ groups can direct both protons toward the same graphite sheet.

Conclusions

Graphite intercalation compounds (GICs) of the type $KC_x(CH_3-NH_2)_y$ have been prepared by in situ methylamination of stage-II $C_{24}K$ and stage-IV $C_{48}K$, and studied by time-of-flight neutron diffraction. As the vapor pressure of methylamine is increased the compounds pass through a rich sequence of staging transitions, in which the regular repeat of n empty graphite layers is progressively filled by intercalant. In these staging transitions we always find that $\Delta n = -1$, even if the transition involves amination/deamination. We therefore observe lower stage *un-aminated* compounds as methylamine is introduced into the starting compounds. In contrast to this, intercalation of K-GICs with smaller molecules, such as ammonia, gives rise to $\Delta n = 0$ transitions. Isotopic substitution of CD_3ND_2 for CD_3NH_2 has enabled us to determine the detailed structure of the fully aminated stage-I and stage-II end compounds, $C_{24}K(CH_3NH_2)_3$ and $C_{48}K(CH_3NH_2)_3$. We find that the interlayer structure is based on *3-fold* coordinated potassium ions, and is relatively insensitive to the stage.

References and Notes

(1) Inagaki, M. *J. Mater. Res*. **1989**, *4*, 1560.
(2) Dresselhaus, M. S.; Dresselhaus, G. *Adv. Phys*. **1981**, *30*, 139.
(3) Charlier, A.; Charlier, M. F.; Fristot, D. *J. Phys. Chem. Solids* **1989**, *50*, 987.
(4) Fischer, J. E.; Thompson, T. E. *Phys. Today* **1978**, *July*, 36.
(5) Fan, Y. B.; Solin, S. A.; Neumann, D. A.; Zabel, H.; Rush, J. J. *Phys. Rev. B* **1987**, *36*, 3386.
(6) Walters, J. K.; Skipper, N. T.; Soper, A. K. *Chem. Phys. Lett*. **1999**, *300*, 444.
(7) Solin, S. A. *J. Phys. IV* **1991**, *1*, 311.
(8) Qian, X. W.; Stump, D. R.; Solin, S. A. *Phys. Rev. B* **1986**, *33*, 5756.
(9) Edwards, P. P. *Phys. Chem. Liq*. **1981**, *10*, 189.
(10) Edwards, P. P. *J. Phys. Chem*. **1984**, *88*, 3772.
(11) Carlile, C. J.; Jamie, I. McL.; Lockhart, G.; White, J. W. *Mol. Phys*. **1992**, *76*, 173.
(12) Boland, B.; Whapham, S. ISIS Experimental Facilities, Rutherford Appleton Laboratory, Didcot, UK, 1992.
(13) Semenovskaya, S. V.; Khachaturyan, K. A.; Khachaturyan, A. G. *Acta Crystallogr*. **1985**, *A41*, 268.